Experimental Gerontology 128 (2019) 110747

Contents lists available at ScienceDirect

Experimental Gerontology

journal homepage: www.elsevier.com/locate/expgero

Network analysis of frailty and aging: Empirical data from the Mexican Health and Aging Study

Carmen García-Peña[a], Ricardo Ramírez-Aldana[b], Lorena Parra-Rodriguez[b], Juan Carlos Gomez-Verjan[b], Mario Ulises Pérez-Zepeda[b], Luis Miguel Gutiérrez-Robledo[c,*]

[a] Head of the Research Division, National Institute of Geriatrics Mexico City, Mexico
[b] Researcher, Research Division, National Institute of Geriatrics Mexico City, Mexico
[c] General Director, National Institute of Geriatrics Mexico City, Mexico

ARTICLE INFO

Section Editor: Eva Grill

Keywords:
Bayesian networks
Biological aging
Complex networks
Frailty
Probabilistic graphical models
Geriatric epidemiology
Social network analysis

ABSTRACT

Background: Frailty remains a challenge in the aging research area with a number of gaps in knowledge still to be filled. Frailty seems to behave as a network, and in silico evidence is available on this matter. Having in vivo evidence that frailty behaves as a complex network was the main purpose of our study.
Methods: Data from the Mexican Health and Aging Study (main data 2012, mortality 2015) was used. Frailty was operationalized with a 35-deficit frailty index (FI). Analyzed nodes were the deficits plus death. The edges, linking those nodes were obtained through structural learning, and an undirected graph associated with a discrete probabilistic graphical model (Markov network) was derived. Two algorithms, hill-climbing (*hc*) and Peter and Clark (*PC*), were used to derive the graph structure. Analyses were performed for the whole population and tertiles of the total FI score.
Results: From the total sample of 10,983 adults aged 50 or older, 43.8% were women, and the mean age was 64.6 years (SD = 9.3). The number of connections increased according to the tertile level of the FI score. As the FI score raised, groups of interconnected deficits increased and how the nodes are connected changed.
Conclusions: Frailty phenomenon can be modeled using a Bayesian network. Using the full sample, the most central nodes were self-report of health (most connected node) and difficulty walking a block, and all deficits related to mobility were very interconnected. When frailty levels are considered, the most connected nodes differ, but are related with vitality, mainly at lower frailty levels. We derived that not all deficits are equally related since clusters of very related deficits and non-connected deficits were obtained, which might be considered in the construction of the FI score. Further research should aim to identify the nature of all observed interactions, which might allow the development of specific interventions to mitigate the consequences of frailty in older adults.

1. Introduction

The aging process is characterized by its variability, leading to various changes in structure and function at different levels of organization, from molecules, cells, and tissues, to physiological systems and environmental interactions (Kriete et al., 2006). Individuals accumulate deficits and increase their vulnerability to stressors at different speeds throughout life, eventually becoming functionally impaired and dependent (Mitnitski et al., 2017a). This not only poses a burden to the individual and their family, but also represents a challenge for public health systems and society.

Once a peak in development is reached by an individual that allows him/her to function in a determined context, a process of decline starts, leading to gradual deterioration and eventually to death (Hoffmann, 2016). An example of the previous statement is what happens with bone density and height, a well-studied phenomenon in aging. Height reaches its peak around the age of twenty and starts to decrease at the age of thirty (Sorkin et al., 1999); sometimes because of osteoporotic fractures, with a wide variation between individuals. Similarly, people of the same age have different health patterns. The theory of biological aging (BA), implies that the presence of complex multi-causal processes determines interactions at different complexity levels, eventually leading to adverse outcomes (Bjorksten and Tenhu, 1990; Mitnitski et al., 2017a).

* Corresponding author at: National Institute of Geriatrics, Periférico Sur No. 2767, Col. San Jerónimo Lídice, Delegación La Magdalena Contreras, Ciudad de México Código Postal 10200, Mexico.
E-mail address: lmgutierrez@inger.gob.mx (L.M. Gutiérrez-Robledo).

https://doi.org/10.1016/j.exger.2019.110747
Received 4 January 2019; Received in revised form 19 September 2019; Accepted 2 October 2019

On the other hand, frailty is recognized as the clinical representation of damage accumulation (Morley et al., 2013; Rodríguez-Mañas et al., 2013). One of the dominant approaches to its operational definition is the frailty index (FI); which has been proposed (Rockwood et al., 2000; Searle et al., 2008) as a system-level measurement to understand and evaluate the heterogeneous nature of the aging process (i.e., empirical evaluation of BA). The so-called deficits are derived from clinical, biological, or social dimensions that operate as a network system and feature complex interactions (Rutenberg et al., 2017) in an individual. Moreover, the FI has been tested in different contexts: as a health assessment tool with clinical data (Rockwood et al., 2011), in laboratory tests (Howlett et al., 2014), and even in animal models (Whitehead et al., 2014). Notwithstanding, it has also been proven useful to characterize socioeconomic inequalities in health within countries (Hajizadeh et al., 2016) and to predict adverse health outcomes (e.g., falls, institutionalization, disability, mortality, etc.). According to Rockwood and Mitnitski (2007), Searle et al. (2008), and Pérez-Zepeda et al. (2016a), a FI with at least 30 variables is capable of predicting adverse health outcomes. In addition, the patterns of the FI are insensitive to the choice and level (biochemical, cellular, organ, functional, or clinical) of the variables included in its construction (Blodgett et al., 2017).

Several theoretical complex network models have been proposed by Farrell et al. (2016), Farrell et al., 2018, Mitnitski et al. (2017b), Mitnitski et al. (2002), Rutenberg et al. (2017), and Taneja et al. (2016) to understand how health deficits connect and interact with each other and to clarify how the FI is associated with death, as a node and as an end-point. In this context, the FI as a model studies an individual as a whole and gives a numerical estimate of BA; the larger the number, the higher the risk of having an adverse outcome. Additionally, the human organism is modeled as a network of interacting nodes which are not evenly interconnected. In this model, aging is not the result of specific processes or diseases or any other time-dependent parameter, but rather an emergent phenomenon that contradicts programmed theories of aging, and the classic linear medical uni-causal paradigm. Other network approaches have also been implemented by (Hidalgo et al., 2009), to analyze phenotypic disease networks. They found that disease progression can be successfully represented and studied by using network methods, offering the potential to enhance our understanding of the origin and evolution of human diseases.

The objectives of the present study are: 1) Analyze from the Mexican Health and Aging Study (MHAS) (Wong et al., 2017), the relationship between the deficits integrating the frailty index and death, through probabilistic graphical models, which model conditional dependences representing them through a graph; 2) Identify which are the more relevant deficits among them all; 3) Identify the relationship and relevance between frailty deficits over different levels (tertiles) of the frailty index.

2. Methods

2.1. Setting and participants

The network analysis is derived from the longitudinal data from the third and fourth waves (2012 and 2015) from the Mexican Health and Aging Study (MHAS) (Wong et al., 2017). In brief, the aims of the MHAS are to examine the aging process and disability burden, to evaluate the effects of individual behaviors, and to compare health dynamics, among other aims. MHAS baseline was nationally representative of the 13 million Mexicans born prior to 1951. A direct interview was sought with each individual and proxy interviews were obtained when poor health or temporary absence precluded a direct interview. A set of questionnaires (e.g., socio-demographic, health-related, cognitive performance, functional status, among others) was applied head-to-head to community-dwelling Mexican older adults over four waves collected in 2001, 2003, 2012, and 2015. We built all deficits from the 2012 wave and obtained mortality using information from the 2015 wave (corresponding to mortality between 2012 and 2015). In the 2012 wave, 15,723 participants were assessed, including 9827 in the follow-up, and 5896 from a refresh sample (including spouses of the chosen individuals, regardless of age), 1209 deaths were reported by 2015.

For the purpose of the present study, we analyzed participants 50 years or older since we consider aging as a lifelong process, and we have already demonstrated that frailty can begin early in life (Pérez-Zepeda et al., 2016b); thus a sample of 14,872 individuals was obtained. We discarded second or third wives or husbands (165 cases) to avoid problems concerning marital status transitions through time; additionally, since independence between individuals is assumed by our models, analyses without these cases were made, finding for all variables that the correlation between couples was low. For the graphical models, we require information of each binary variable. Thus, we discarded cases with missing values in any variable, and from a total of 14,707 cases, a final sample of 10,983 was retained for the present analysis. It is important to notice that it is possible to calculate the FI associated with cases without all variables. However, Bayesian network analysis requires the values associated with each component of the FI.

3. Variables

3.1. Frailty

A set of 35 variables (deficits) was included, as determined by Searle et al. (2008), as criteria (all self-reported data). Variables were related to functional status, chronic diseases, self-rated health, cognitive status, and depressive symptoms.

Most chosen variables contained categories "Yes" and "No," and some had two additional categories corresponding to "can't" or "doesn't do." These categories were properly assigned; for instance, for the question "Because of a health problem, do you have difficulty dressing yourself?" we considered that when a person answered "can't" or "doesn't do", a deficit was present. From the total of 35 deficits, each individual had an FI score that was estimated as follows: sum of deficits/35, with scores going from zero (lowest frailty burden possible) to one (highest frailty burden possible). Cut-off points and deficits included are presented in Table 1. The syntaxes used to generate all variables are shown in Appendix 1 (Supplementary section).

In order to stratify by frailty level, tertiles of the total score of the FI were obtained. Since there is not a consensus about how to define biologically pertinent categories, we decided not to build the network over a clinical pre-conception, and to use tertiles as natural cut-off points that emerge from the data. The first tertile corresponds up to 0.11 and the second goes up to 0.20.

3.2. Mortality

Mortality from 2012 to 2015 was recovered from cumulative data associated with wave 2015.

3.3. Analytic plan

A data set corresponding to all deficits in 2012 and mortality between 2012 and 2015 was built. Since our analyses are based on probabilistic graphical models (Lauritzen, 1996), we first define the 35 deficits and mortality variables as vertices or nodes (which we graphically represent in this paper by ellipses, set V). The edges (graphically represented by lines), or ties, linking those nodes (set E) were obtained from our data through structural learning. Structural learning allows us to obtain through algorithms the probabilistic relationship between variables and a corresponding graph from observed data. Hence, an undirected discrete graph G (V, E) (Bondy and Murty, 1976) associated with a Markov network (a discrete graphical probabilistic

Table 1
Cut points, frequency of deficits and tertiles of frailty.

Variable description (name)	All cases N = 10,983 Frequency (%)	Frailty level FI = 0–0.11 0–4 deficits First tertile N = 4747 Frequency (%)	FI = 0.12–0.20 5–7 deficits Second tertile N = 2649 Frequency (%)	FI > 0.20 deficits ≥ 8 Third tertile N = 3587 Frequency (%)
Help dressing	983 (8.95)	25 (0.53)	90 (3.40)	868 (24.20)
Help getting in/out of a chair	3264 (29.72)	342 (7.20)	697 (26.31)	2225 (62.03)
Help walking around the room	160 (1.46)	1 (0.02)	4 (0.15)	155 (4.32)
Help eating	101 (0.92)	1 (0.02)	4 (0.15)	96 (2.68)
Help grooming	150 (1.37)	0	2 (0.08)	148 (4.13)
Help using toilet	128 (1.17)	0	4 (0.15)	124 (3.46)
Help up/down one flight of stairs	2594 (23.62)	148 (3.12)	465 (17.55)	1981 (55.23)
Help lifting 10 lbs	2557 (23.28)	174 (3.67)	430 (16.23)	1953 (54.45)
Help shopping groceries	865 (7.88)	28 (0.59)	58 (2.19)	779 (21.72)
Help with preparing a hot meal	630 (5.74)	90 (1.90)	97 (3.66)	443 (12.35)
Help taking medication	162 (1.48)	2 (0.04)	5 (0.19)	155 (4.32)
Help with finances	169 (1.54)	6 (0.13)	9 (0.34)	154 (4.29)
Compared to 2 years ago: change in weight	2375 (21.62)	543 (11.44)	597 (22.54)	1235 (34.43)
Poor/regular self-rated health	1315 (11.97)	27 (0.57)	149 (5.62)	1139 (31.75)
Compared to 2 years ago much worst/worst self-rated health	3149 (28.67)	352 (7.42)	737 (27.82)	2060 (57.43)
Last 12 months: number of days in bed… due to sickness/injury	1941 (17.67)	321 (6.76)	447 (16.87)	1173 (32.70)
Within the past week: felt tired	6402 (58.29)	1535 (32.34)	1783 (67.31)	3084 (85.98)
Difficulty walking a block	1353 (12.32)	29 (0.61)	144 (5.44)	1180 (32.90)
Feel everything is an effort	3810 (34.69)	460 (9.69)	866 (32.69)	2484 (69.25)
Feel depressed	3705 (33.73)	347 (7.31)	937 (35.37)	2421 (67.49)
Feel happy	2187 (19.91)	214 (4.51)	456 (17.21)	1517 (42.29)
Feel lonely	3196 (29.10)	392 (8.26)	803 (30.31)	2001 (55.78)
Feel energetic	5639 (51.34)	1522 (32.06)	1487 (56.13)	2630 (73.32)
Hypertension/high blood pressure	4727 (43.04)	1154 (24.31)	1235 (46.62)	2338 (65.18)
Heart attack	378 (3.44)	34 (0.72)	83 (3.13)	261 (7.28)
Heart failure	207 (1.88)	9 (0.19)	36 (1.36)	162 (4.52)
Stroke	203 (1.85)	17 (0.36)	34 (1.28)	152 (4.24)
Cancer (in the last 10 years)	227 (2.07)	42 (0.88)	56 (2.11)	129 (3.60)
Diabetes	2394 (21.80)	510 (10.74)	603 (22.76)	1281 (35.71)
Arthritis/rheumatism	1490 (13.57)	188 (3.96)	319 (12.04)	983 (27.40)
Respiratory illness	639 (5.82)	94 (1.98)	134 (5.06)	411 (11.46)
Compared to 2 years ago: respondent reports his/her memory quality	2342 (21.32)	325 (6.85)	543 (20.50)	1474 (41.09)
Respondent's dominant hand strength	2566 (23.36)	211 (4.44)	550 (20.76)	1805 (50.32)
Anorexia: last 2 years: loss of appetite	515 (4.69)	41 (0.86)	87 (3.28)	387 (10.79)
Exercise: last 2 years: exercise or hard physical work ≥ 3 times a week	6647 (60.52)	2259 (47.59)	1693 (63.91)	2695 (75.13)
Died between 2012 and 2015	574 (5.23)	109 (2.30)	115 (4.34)	350 (9.76)

model; (Agresti, 2012)) can be derived (Appendix 2). In these models, the lack of an edge (or a line) between two variables means that the two variables are conditionally independent given the other variables.

Since the number of vertices in our data was too large, structural learning was possible by using two of the most used algorithms designed for larger graphs associated with directed graphical probabilistic models (Bayesian networks), hill-climbing (*hc*) and Peter and Clark (*PC*) algorithms (Heckerman et al., 1995; Højsgaard et al., 2012; Spirtes and Glymour, 1991). The former is based upon a score optimization and the latter on a series of hypothesis tests concerning conditional independence (for more details see Appendix 2). From the *hc* algorithm, a directed graph (directed acyclic graph or *DAG*) was obtained; however, since we need an undirected graph preserving the same conditional and marginal independences as in the *DAG*, we applied the so-called *moralization* (a process used in graph theory) of the *DAG*. From the *PC* algorithm, the undirected graph is directly obtained. For the structural learning process with the *hc* algorithm, we used the Bayesian Information Criterion (BIC) and specified zero random restarts (a number used to avoid a local optimum when optimizing the score), as scores. For the *PC* algorithm, conditional independence tests are required, and since we are analyzing deficits, we defined that the tests corresponded to binary variables using a log-likelihood ratio test and a significance level of 0.05. No edges were forbidden or forced to appear with any algorithm, thus, not allowing any preconception. To see the robustness of the results obtained, some of these default values were modified, and the resulting models were not too different (e.g., using the Bayesian Dirichlet score, BDe, with the “e” for likelihood-equivalence, instead of BIC score and three random restarts, 95.28% of the edges in the original model were preserved).

In order to compare with simpler models, we applied a pairwise correlation approach and obtained the correlation plot based on Pearson correlation by using the CorrPlot package from R. The statistical software, R-studio (R-version 3.3), was used through the bnlearn (Scutari, 2009) and pcalg (Kalisch et al., 2012) packages to implement in our data set (without missing values) the *hc* and *PC* algorithms, respectively.

Using the aforementioned processes, four graphs were obtained from each algorithm, one for all observations and three corresponding to the frailty levels obtained from the tertiles (eight graphs in total). The first frailty level corresponds to an FI from 0 to 0.11 (0 to 4 deficits), the second frailty level corresponds to an FI from 0.12 to 0.20 (5 to 7 deficits), the third frailty level corresponds to an FI greater to 0.20 (8 or more deficits).

We used both, *hc* and *PC* algorithms, to see the robustness of the obtained relationships, the associated graph obtained from the *PC* algorithm would typically have fewer edges. Technical details of graphical models and algorithms are explained in Appendix 2.

In the graphs (Figs. 1 to 4), each node represents either a frailty deficit or death. If a node has many edges with other nodes, then there is more dependence among them. In these networks, the association is

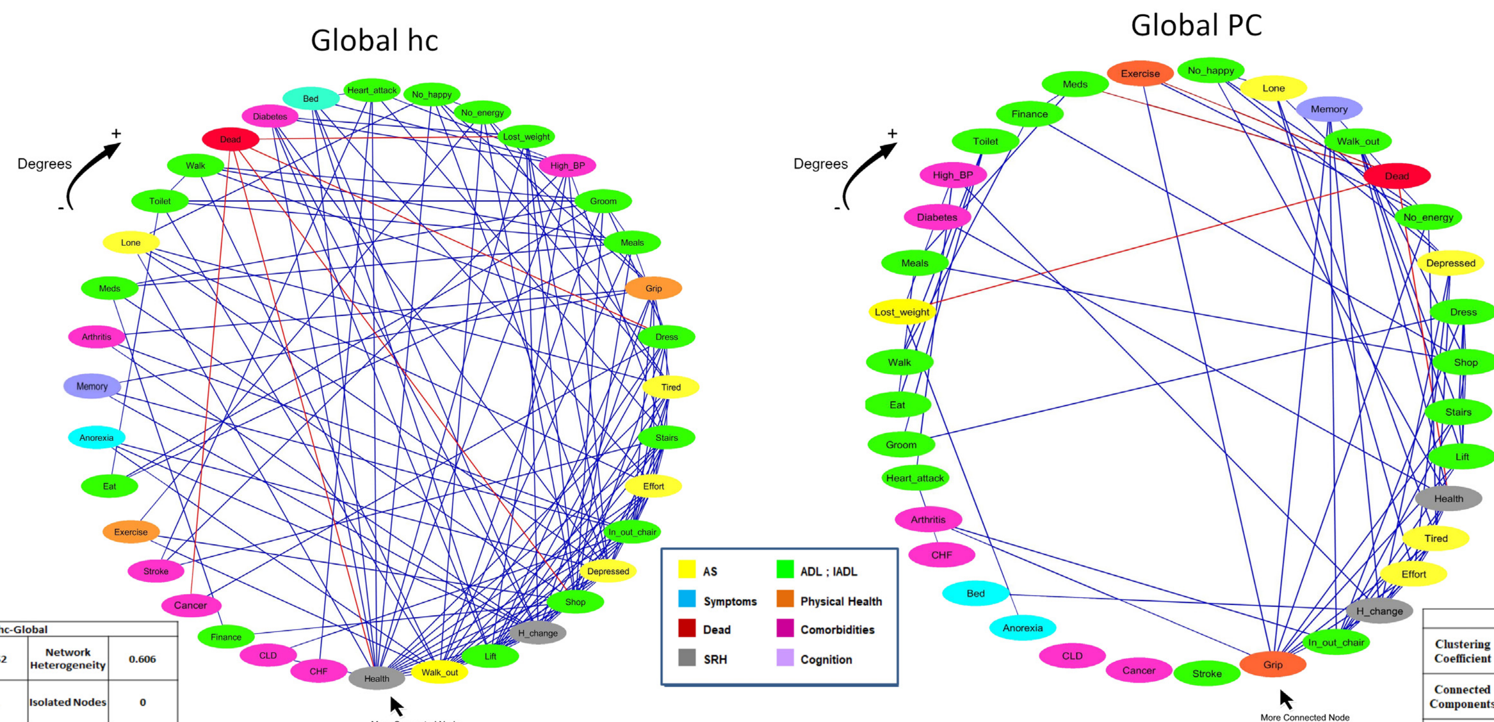

hc-Global			
Clustering Coefficient	0.652	Network Heterogeneity	0.606
Connected Components	1	Isolated Nodes	0
Network Centralization	0.326	Shortest Paths	1260 (100%)
Avg. Number of Neighbors	7.222	Network Density	0.206

PC -Global			
Clustering Coefficient	0.179	Network Heterogeneity	0.624
Connected Components	4	Isolated Nodes	3
Network Centralization	0.158	Shortest Paths	1056(83%)
Avg. Number of Neighbors	3.778	Network Density	0.108

Fig. 1. Network constructed for frailty deficits associated with *hc* and *PC* algorithms for all observations. Each node represents a frailty deficit or death. The absence of an edge between two nodes means that the associated random variables are conditionally independent given the remaining variables. If a node has many edges with other nodes, then there is more dependence among them. Nodes are arranged clockwise from less connected to most connected node. Nodes are colored by classification (see below) and edges are colored in red for those deficits connecting with dead. Below each figure there is a table with some of the most important properties of the network (see Analytic plan).

Nodes are colored according to the following classification: Yellow-AS (Affective Status: No Happy, Lone, No energy, Depressed, Tired, Effort); Light Blue-Symptoms (Anorexia, Bed, Lost of weight); Red-Dead; Gray-SRH (Self-rated health: Health, H_change); Green-ADL-IADL (activities of daily living and Instrumental activities of daily living: In_out_chair, Stairs, Lift, Shop, Dress, Walk, Eat, Groom, Meals, Meds, Finance Toilet); Orange-Physical Health (Grip, Exercise); Pink (CLD, Stroke, Cancer, CHF, Arthritis, Heart_Attack, Diabetes, High_BP); Navy Blue-Cognition (Memory). (For interpretation of the references to color in this figure legend, the reader is referred to the web version of this article.)

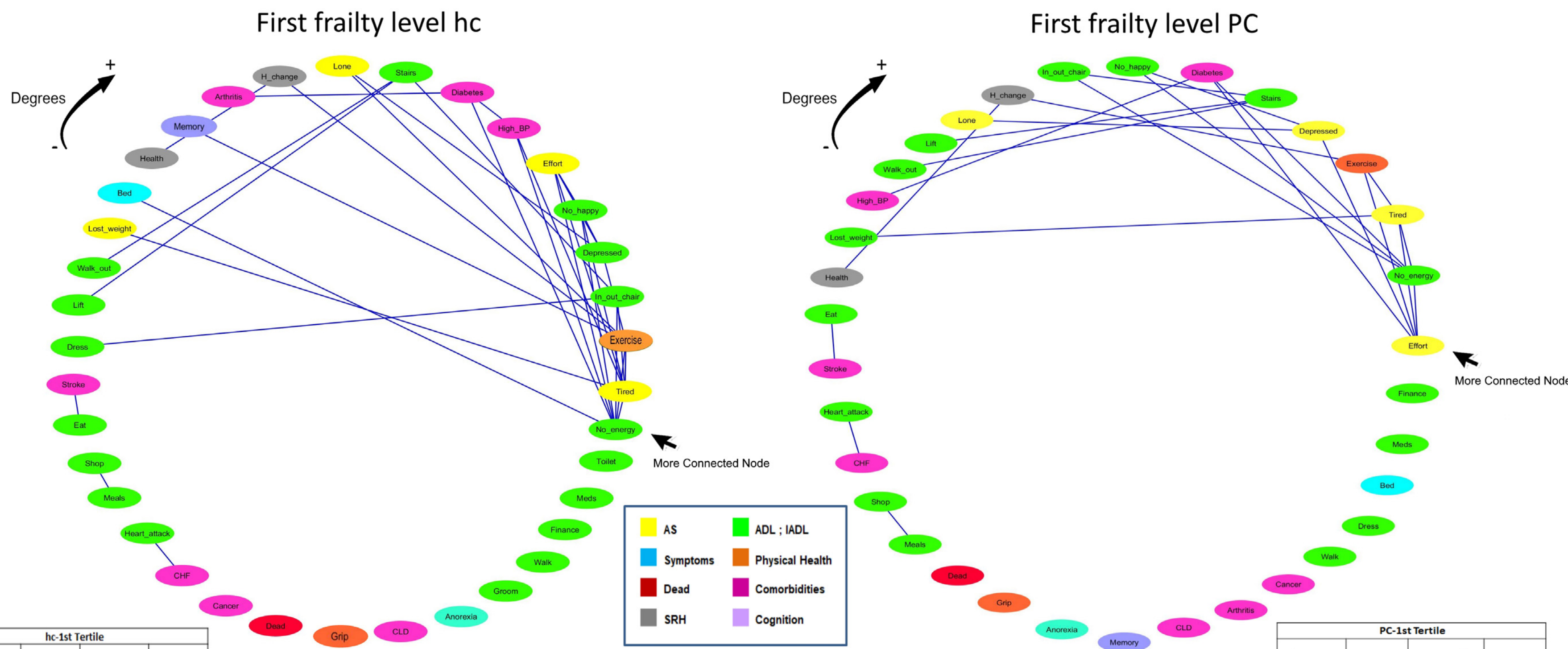

hc-1st Tertile			
Clustering Coefficient	0.125	Network Heterogeneity	1.141
Connected Components	14	Isolated Nodes	10
Network Centralization	0.188	Shortest Paths	386 (30%)
Avg. Number of Neighbors	1.778	Network Density	0.051

PC-1st Tertile			
Clustering Coefficient	0.044	Network Heterogeneity	1.110
Connected Components	16	Isolated Nodes	12
Network Centralization	0.119	Shortest Paths	246 (21%)
Avg. Number of Neighbors	1.294	Network Density	0.039

Fig. 2. Network constructed for each frailty deficits associated with *hc* and *PC* algorithms for the first tertile. Each node represents a frailty deficit or death. The absence of an edge between two nodes means that the associated random variables are conditionally independent given the remaining variables. If a node has many edges with other nodes, then there is more dependence among them Nodes are arranged clockwise from less connected to most connected node. Nodes are colored by classification (see below) and edges are colored in red for those deficits connecting with dead. Below each figure there is a table with some of the most important properties of the network (see Analytic plan). Check on-line image and supplementary information for more details.
Nodes are colored according to the following classification: Yellow-AS (Affective Status: No Happy, Lone, No energy, Depressed, Tired, Effort); Light Blue-Symptoms (Anorexia, Bed, Lost of weight); Red-Dead; Gray-SRH (Self-rated health: Health, H_change); Green-ADL-IADL (activities of daily living and Instrumental activities of daily living: In_out_chair, Stairs, Lift, Shop, Dress, Walk, Eat, Groom, Meals, Meds, Finance Toilet); Orange-Physical Health (Grip, Exercise); Pink (CLD, Stroke, Cancer, CHF, Arthritis, Heart_Attack, Diabetes, High_BP); Navy Blue-Cognition (Memory). (For interpretation of the references to color in this figure legend, the reader is referred to the web version of this article.)

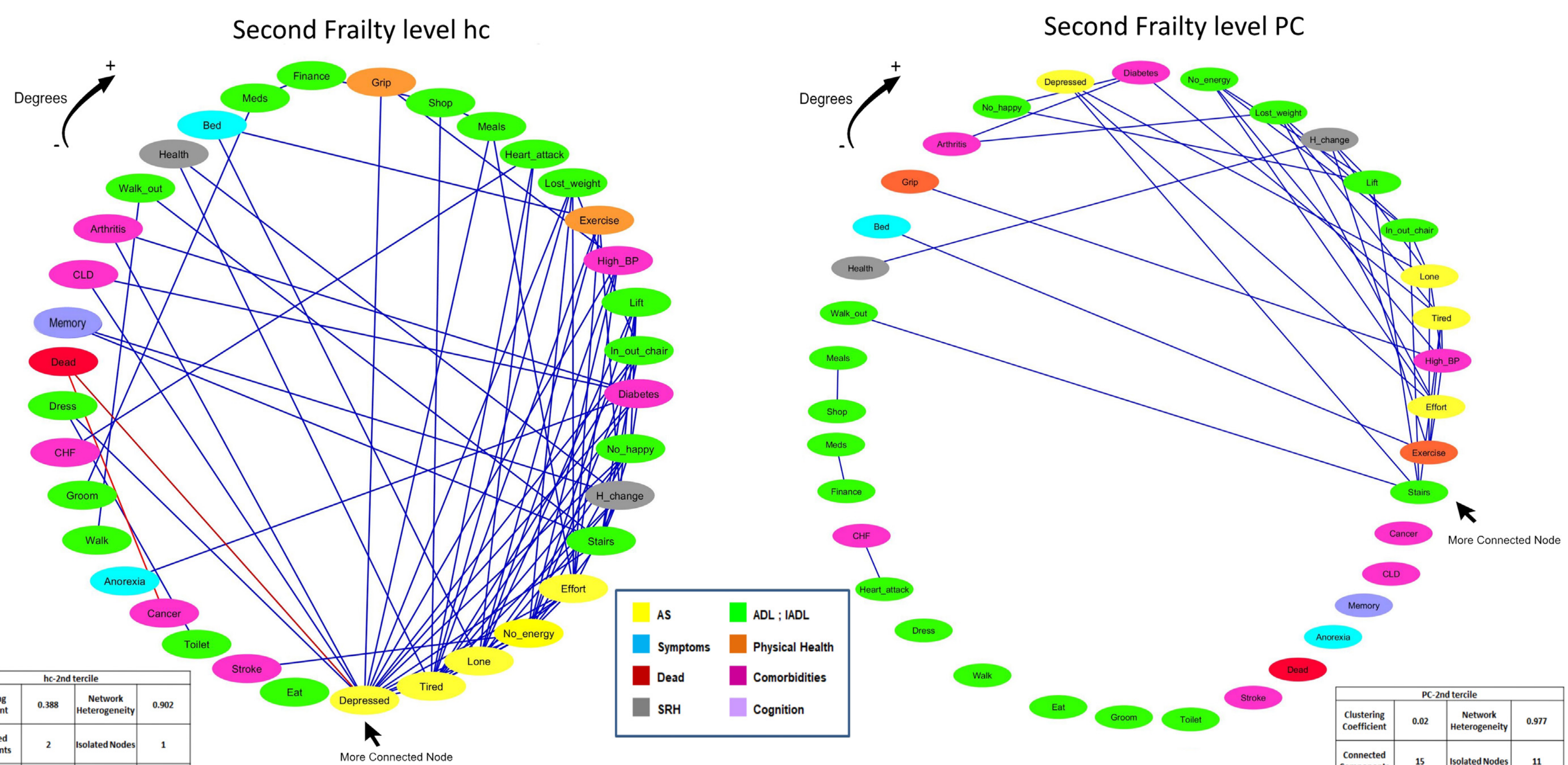

hc-2nd tercile			
Clustering Coefficient	0.388	Network Heterogeneity	0.902
Connected Components	2	Isolated Nodes	1
Network Centralization	0.356	Shortest Paths	1190 (94%)
Avg. Number of Neighbors	4.222	Network Density	0.121

PC-2nd tercile			
Clustering Coefficient	0.02	Network Heterogeneity	0.977
Connected Components	15	Isolated Nodes	11
Network Centralization	0.092	Shortest Paths	348 (27%)
Avg. Number of Neighbors	1.944	Network Density	0.056

Fig. 3. Network constructed for each frailty deficits associated with *hc* and *PC* algorithms for the second tertile. Each node represents a frailty deficit or death. The absence of an edge between two nodes means that the associated random variables are conditionally independent given the remaining variables. If a node has many edges with other nodes, then there is more dependence among them. Nodes are arranged clockwise from less connected to most connected node. Nodes are colored by classification (see below) and edges are colored in red for those deficits connecting with dead. Below each figure there is a table with some of the most important properties of the network (see Analytic plan). Check on-line image and supplementary information for more details.
Nodes are colored according to the following classification: Yellow-AS (Affective Status: No Happy, Lone, No energy, Depressed, Tired, Effort); Light Blue-Symptoms (Anorexia, Bed, Lost of weight); Red-Dead; Gray-SRH (Self-rated health: Health, H_change); Green-ADL-IADL (activities of daily living and Instrumental activities of daily living: In_out_chair, Stairs, Lift, Shop, Dress, Walk, Eat, Groom, Meals, Meds, Finance Toilet); Orange-Physical Health (Grip, Exercise); Pink (CLD, Stroke, Cancer, CHF, Arthritis, Heart_Attack, Diabetes, High_BP); Navy Blue-Cognition (Memory). (For interpretation of the references to color in this figure legend, the reader is referred to the web version of this article.)

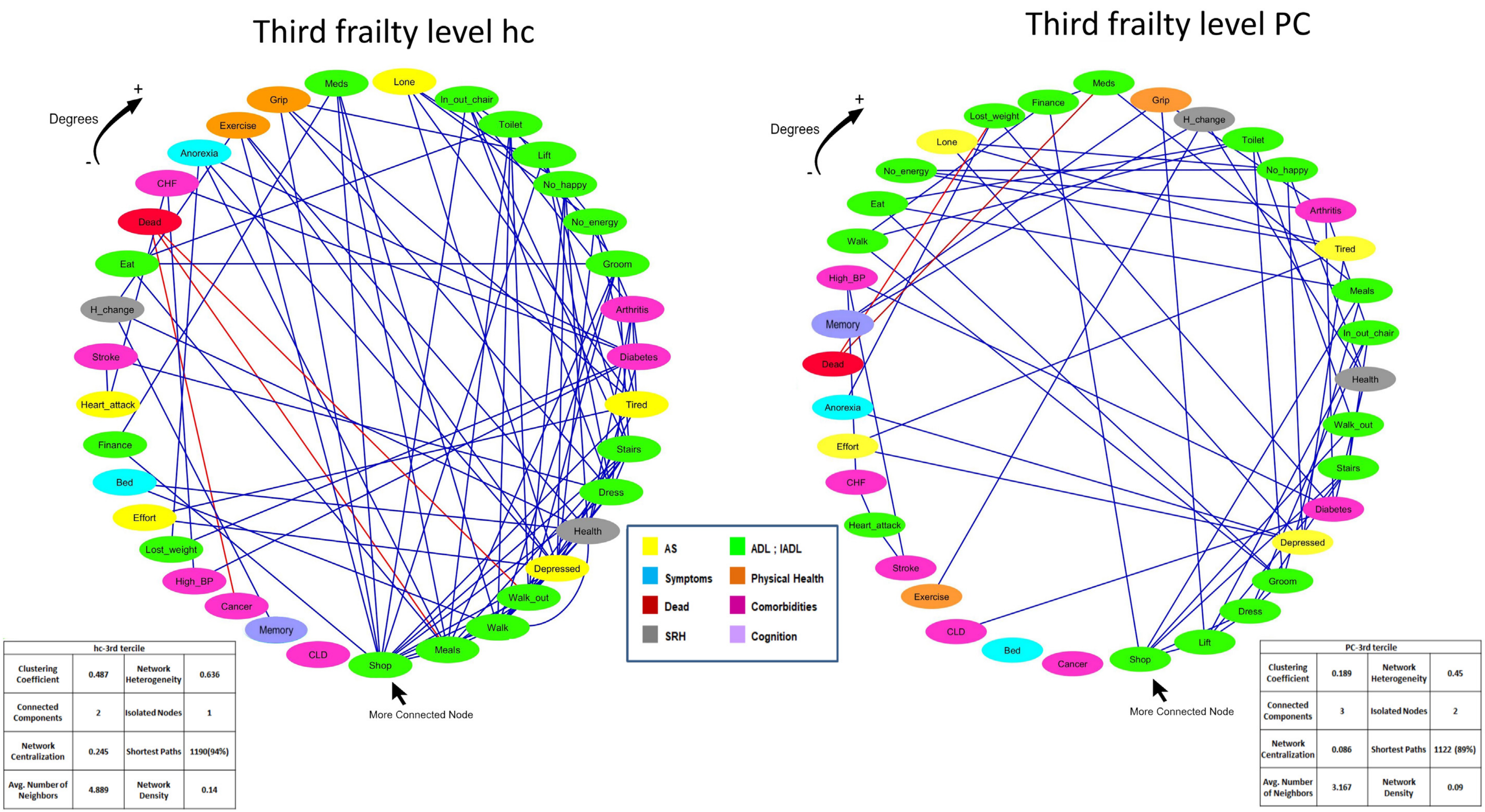

hc-3rd tercile			
Clustering Coefficient	0.487	Network Heterogeneity	0.636
Connected Components	2	Isolated Nodes	1
Network Centralization	0.245	Shortest Paths	1190(94%)
Avg. Number of Neighbors	4.889	Network Density	0.14

PC-3rd tercile			
Clustering Coefficient	0.189	Network Heterogeneity	0.45
Connected Components	3	Isolated Nodes	2
Network Centralization	0.086	Shortest Paths	1122 (89%)
Avg. Number of Neighbors	3.167	Network Density	0.09

Fig. 4. Network constructed for each frailty deficits associated with *hc* and *PC* algorithms for the third tertile. Each node represents a frailty deficit or death. The absence of an edge between two nodes means that the associated random variables are conditionally independent given the remaining variables. If a node has many edges with other nodes, then there is more dependence among them. Nodes are arranged clockwise from less connected to most connected node. Nodes are colored by classification (see below) and edges are colored in red for those deficits connecting with dead. Below each figure there is a table with some of the most important properties of the network (see Analytic plan).
Nodes are colored according to the following classification: Yellow-AS (Affective Status: No Happy, Lone, No energy, Depressed, Tired, Effort); Light Blue-Symptoms (Anorexia, Bed, Lost of weight); Red-Dead; Gray-SRH (Self-rated health: Health, H_change); Green-ADL-IADL (activities of daily living and Instrumental activities of daily living: In_out_chair, Stairs, Lift, Shop, Dress, Walk, Eat, Groom, Meals, Meds, Finance Toilet); Orange-Physical Health (Grip, Exercise); Pink (CLD, Stroke, Cancer, CHF, Arthritis, Heart_Attack, Diabetes, High_BP); Navy Blue-Cognition (Memory). (For interpretation of the references to colour in this figure legend, the reader is referred to the web version of this article.)

not measured by pairs through a correlation but through a decomposition of the joint probability, representing in a more precise way the relationship among all variables.

Each graph contains graphical statistical properties associated with it and colored nodes representing groups, nodes are arranged clockwise from less connected to most connected node starting from below (in each figure it is indicated the most connected node). Nodes are colored according to the following classification: Yellow-AS (Affective Status: No Happy, Lone, No energy, Depressed, Tired, Effort); Light Blue-Symptoms (Anorexia, Bed, Lost of weight); Red-Dead; Gray-SRH (Self-rated health: Health, H_change); Green-ADL-IADL (activities of daily living and Instrumental activities of daily living: In_out_chair, Stairs, Lift, Shop, Dress, Walk, Eat, Groom, Meals, Meds, Finance Toilet); Orange-Physical Health (Grip, Exercise); Pink (CLD, Stroke, Cancer, CHF, Arthritis, Heart_Attack, Diabetes, High_BP); Navy Blue-Cognition (Memory). Edges are colored in red for those deficits connecting with dead.

Below each figure, there is a table with some of the most important properties of the network. Such properties are clustering coefficient (the number of closed triplets, or 3 × triangles, over the total number of triplets), network heterogeneity (reflects the tendency of a network to contain hub nodes), connected components (a maximal set of nodes such that each pair of nodes is connected by a path), isolated nodes (a connected component with only one vertex), network centralization (measure of how much the degree of every node is far from the degree of the highest degree node), shortest paths (how many paths between any two pairs of nodes in the network have the fewest number of links), average number of neighbors, and network density (comparison between the edges available in a graph and a graph with all possible edges). At the top of figure and table, we indicate the algorithm and sample used to obtain each network.

Additionally, the following centrality measures used in social network analysis are calculated for each node and are included in Appendices 3 and 4: degree of the graph (k, number of edges connected to the node), betweenness centrality (C_B, extent to which a node sits "between" pairs of other nodes in the network, such that a path between other nodes has to go through that node), and closeness centrality (C, inverse of the sum of all distances between node i and all other nodes in the network).

4. Results

From the total sample (n = 10,983), 56.21% were women (n = 6173). The mean age was 64.58 years (SD = 9.26, R = 50–102). The number of deaths between 2012 and 2015 was 574 (5.23%). The mean FI, considering all observations was 0.18 (SD = 0.13, R = 0–0.80).

The description, cut-off values for each deficit, number and percentage of participants with deficits in the total sample and by frailty tertile are presented in Table 1. Deficits with the higher percentage of participants were those related with mobility (help in/out of a chair = 29.72%, help up/down one flight of stairs = 23.62%, and help lift ten pounds = 23.28%). Also, components of the depression scale resulted in high percentages (feel depressed = 33.73% and feel lonely = 29.10%). In participants, 43.04% reported a diagnosis of hypertension and 21.80% reported a diagnosis of diabetes. Physical inactivity was present in 60.52% (Table 1).

Appendices 3 and 4 show three centrality measures: degree, betweenness, and closeness, and connected variables in the full sample and by frailty tertile in the *hc* and *PC* algorithms. The number of connections increased according to the level of frailty. Groups of deficits were connected; these groups get larger as the level of frailty increases. Almost all deficits related to mobility were interconnected, particularly those variables that indicated severe impairment. Such was the case for help getting dressed, using the toilet and bathing. On the other hand, mental health deficits connected with each other as well.

The graphs obtained by using both the *hc* and *PC* algorithms are presented in Figs. 1 to 4. Fig. 1 corresponds to the graphical models associated with people 50 years and older, using the *hc* and *PC* algorithms for all observations. The network obtained from the *hc* algorithm does not have any non-connected nodes, and the most connected nodes are self-rating of health with 18 connections, difficulty walking a block with 16 connections, help lifting 10 pounds and report of current health comparison to two years ago, both with 14 connections.

Apart from the number of connections (degree), the other two centrality measures, betweenness and closeness, can be used to determine the most relevant nodes. Considering the *hc* algorithm, the greatest values associated with these two measures corresponded also to self-rating of health and difficulty walking a block (betweenness of 0.18 and closeness of 0.66 for the former, and betweenness of 0.21 and closeness of 0.64 for the latter, Appendix 3), which means that these are the most central nodes (hubs) in the network.

Figs. 2, 3 and 4 correspond to graphical models associated with each of the three frailty levels. An increase in the number of connections was steady, according to the level of frailty, but the graph for the full sample had a higher number of connections.

Considering the *hc* algorithm, the network corresponding to the first level of frailty (Fig. 2) presented eight non-connected nodes: help walking around the room, managing medicines, managing finances, cancer, lung disease, self-reported handgrip strength, anorexia, and death. Therefore, for the people with the lowest level of frailty, these nodes were independent of all the other nodes. Additionally, three dumbbells arose: eat-stroke, shop-meals, and heart attack-chronic heart failure. Hence, each one of these pairs was dependent among themselves but independent from all the other deficits. The most-connected nodes in this case were not feeling energetic, tiredness, and not doing exercise or hard work regularly, with 8, 7, and 6 connections respectively. All of them related to feeling the need to rest.

For the network corresponding to the second level of frailty (Fig. 3) and obtained from the *hc* algorithm, there was only one independent node: help with eating. The most connected nodes were feeling depressed, feeling tired, and feeling that everything is an effort with 16, 14, and 9 edges, respectively. For the network corresponding to the highest level of frailty and obtained from the *hc* algorithm (Fig. 4), there was one non-connected node, which was lung disease, while the most-connected nodes were help shopping groceries with 13 edges, help with preparing hot meals with 11 connections, and help walking around a room and difficulty walking a block both with 10 edges.

Connection with death happened first in the second frailty level with depression and cancer, and in the highest frailty level with critical basic ADLs like difficulty walking a block and help with preparing hot meals as well as cancer.

5. Discussion

In this study, we were able to model the frailty components and mortality with data corresponding to a Mexican aging study as a probabilistic graphical model. We identified that self-report of health and difficulty walking a block are the most relevant nodes, since they are the most connected nodes, nearest to other nodes, and can be considered as intermediaries between all nodes. This means that these nodes are more relevant than others when defining the FI, and such importance could be considered in the index calculation. We also observed that mobility nodes are very interconnected, hence, there is a lot of dependence between them, forming even perhaps a cluster. For the two lowest frailty levels, nodes related with vitality were the most relevant and there were a lot of non-connected nodes, which means that the answer provided by individuals corresponding to vitality are more or less independent to the ones in other questions, being these vitality nodes central when clusters of probabilistic dependence are formed with variables related with them.

Network approaches help us to analyze the complex phenomena and dynamics of aging (Network Theory of Aging) (Kowald and Kirkwood, 1994; Kriete et al., 2006), as well as to understand the origin and evolution of human diseases (Hidalgo et al., 2009). In the present study, we performed a network analysis based on empirical data from MHAS; in order to increase the knowledge on the nature of frailty as a network. To the best of our knowledge, this is the first report using actual empirical data approached by probabilistic graphical models in the field of frailty research. Our findings suggest a trend towards deterioration with increasing levels of the frailty index that contributes to clarifying the specific nature of each node integrating the FI in the successive stages of frailty. This also adds to what is already known about frailty dynamics according to severity levels. There is a wide variety of possible interactions between the deficits that integrate an FI. These connections vary according to incremental scores of the FI. It is worth noting that the characteristics of the FI used in this study are similar to those previously reported regarding associated risks. The higher the FI score, the higher the mortality, however, our network analysis results differ from those previously reported from in silico simulations (Farrell et al., 2016; Mitnitski et al., 2017b; Rutenberg et al., 2017; Taneja et al., 2016), since our methodology was based on the information of all individuals to build a network representing in our case an emerging feature: the joint probability distribution and associations between variables by using Bayesian networks, in contrast with the methodology used by Mitnitski et al., where they simulated a network for each individual according to the theoretical connections that all deficit and death nodes could have.

It is important to notice that the networks obtained from the stochastic model of interacting deficits proposed previously (Farrell et al., 2016; Taneja et al., 2016) and the networks resulting from the graphical model that we present here, are based on different approaches and therefore the interpretation of the graphs is different. Our approach describes the emerging properties derived from the cumulative information coming from a representative sample of a population with 35 frailty deficits and a mortality node. Within our network, nodes represent the deficits while edges represent dependencies. For example, nodes that are not connected represent deficits that are conditionally independent of each other given the rest of the variables. Unlike the previous approach (Farrell et al., 2016; Taneja et al., 2016), the mortality node in this network is not the most connected node, but the deficits that are connected with death are the ones that influence this outcome for the individuals represented in the network.

Our approach shows that the interactions within deficits vary according to increasing values of the FI score. As the FI increases, the complexity of the network and the number of connections progressively increase. Interestingly, there is no relationship between the frequency of a deficit and the number of connections. In addition, the progression of the connected nodes in the different tertiles shows a downward gradient of decreasing vitality.

When analyzing how deficits interact with each other, some other conclusions could be drawn that merit further testing. As already stated by Lipsitz (Lipsitz, 2016), it is still not clear if frailty results from the loss of complexity in the interactions of its nodes, independently of which specific nodes are interacting, and it is a matter of study how and at what rates deficits aggregate. The nodes integrating the frailty index have different and probably specific meanings and interacting pathways. FI seems to change each year of age between 3 and 6% in both human and murine models. (Rockwood and Howlett, 2019). Nevertheless, there is no certainty on the nature of individual deficits, for example, if an individual has an FI of ≥ 0.7, the addition of one more deficit would lead to death, regardless of the added deficit.

The network obtained under the *PC* algorithm provides fewer edges than those obtained through the *hc* algorithm (Appendix 2). The real dependence among all variables, which is what we are modelling, lies between the dependence obtained from both algorithms. Hence, the *hc* and *PC* methods were used to prove the robustness of our results.

Almost all edges from the *PC* algorithm are preserved when compared with the *hc* algorithm. When using all the observations, 88.24% of the edges obtained through the *hc* algorithm were the same as the ones obtained from the *PC* algorithm, which is a robust finding (shared edges are marked in Appendices 3 and 4, and the comparison between shared edges is shown in Appendix 5). Interestingly, independently of the algorithm used, there is a change between deficit connections for the different frailty groups; moreover, not all deficits have the same importance in the network.

Regarding the two algorithms, *hc* and *PC*, the most connected node shared by both algorithms in the global network is report of current health comparison to two years ago. For the other frailty levels, they are: 1st frailty level (not feeling energetic, tiredness), 2nd. Frailty level (tiredness and feeling that everything is an effort), and 3rd Frailty Level (help shopping groceries). The most connected nodes shared by both algorithms could be characterized as the more relevant in our findings, interacting with a greater number of deficits.

According to our study, FI shows different levels of conditional probabilistic dependence, and specific deficits seem to act synergistically in the presence of others. Using the *hc* algorithm, for example, one of the most connected nodes is self-perception of health in the global network. Lack of energy, feeling tired, not exercising, and needing help walking around the room are the most connected nodes in the first, second and third level of frailty. The constant presence of these variables adds to the hypothesis of decreasing vitality (energy management blockade) and consecutive functional impairment underlying the frailty trajectory. Besides, the feeling of autonomy (associated with an internal control locus) leads to a higher subjective wellbeing. In this context, vitality and autonomy could be more important for health than the presence of chronic diseases (Abizanda et al., 2016; Geisler et al., 2016).

In addition, a worsening intrinsic capacity correlates with lack of energy and vitality (Zengarini et al., 2015, 2016) and it could be seen how dependency and need for care arise. There is not only low energy, but specific clinical implications that have a significant impact on functional ability leading to dependency and need for care. In fact, available evidence suggests that the higher the levels of frailty measured with the FI, the higher the resting metabolic rate, pointing to an overall disruption of energy metabolism in older adults (Kim et al., 2014). In addition, both frailty and abnormal energy metabolism have been related to decreased muscle mass and function, a potential area of intervention. It could be argued that these deficits will not universally appear in other populations or even in the same cohort over time. Notwithstanding, as previously stated, energetic disruptions seem to be a constant in the aging individual and could be a plausible explanation to our findings.

It is important to notice that the edges in undirected discrete networks are not obtained from a correlation matrix. They are derived through a decomposition of the probability associated with all variables at the same time according to independence relationships (marginal and conditional). Additionally, the *hc* algorithm is based on a score. Thus, a threshold defining a level of association between variables is not necessary: the data and the edges added or deleted are enough to iteratively calculate the score. Hence, structural learning through scores is not dependent on correlations. For instance, for a correlation coefficient above 0.6, the resulting network has only two edges (Fig. 5), resulting in a completely different network from the ones obtained before. For the *PC* algorithm, statistical tests associated with conditional independences and a fixed significance level of 0.05 are used. Hence, a "distance" or "association" measure between nodes is also unnecessary.

Frailty is still a matter of discussion in the aging research area. One of the main current controversies relates to the operationalization of this condition and its implications both at the individual and population health levels. Reaching a full understanding of the mechanisms behind deficit interactions and recognizing the most important deficits (i.e. most and less connected nodes in the network) will allow us to move forward towards the development of interventions to prevent or alleviate frailty.

However, several issues remain to be clarified with ongoing research. All the variables included in the FI were obtained by self-report, and the interactions could be influenced by how the questions were formulated. Another flaw is that even though interactions among nodes differ in the FI tertiles, we are yet to prove that there is a precise trajectory when we observe the behavior of the network over a time frame. A longitudinal study of the trajectories of these interactions is ongoing in order to clarify this issue.

The emerging needs of frail older people continue to grow and already flood our clinical services. There is an urgent need for a deeper understanding of the phenomenon in order to develop newer approaches that lead to better solutions for their care. Complex network analysis is one of these new approaches. Its relevance has been demonstrated when applied to other disciplines, and it has provided essential solutions (Kalisch et al., 2012). Future research must be focused on the true meaning of the possible interactions that we propose. A deeper understanding of the interplay of interactions between deficits, and its change over time, is also needed in order to reach an understanding about the resulting trajectories.

Supplementary data to this article can be found online at https://doi.org/10.1016/j.exger.2019.110747.

Funding

We declare no competing interests. This project was supported by a grant from the Secretaría de Ciencia, Ciudad de México SECITI 042/2018 "Red colaborativa de Investigación Traslacional para el Envejecimiento Saludable de la Ciudad de México (RECITES).

References

Abizanda, P., Romero, L., Sánchez-Jurado, P.M., Ruano, T.F., Ríos, S.S., Sánchez, M.F., 2016. Energetics of aging and frailty: the FRADEA Study. J. Gerontol. Ser. A Biol. Med. Sci. 71 (6), 787–796.
Agresti, A., 2012. Categorical Data Analysis, 3rd edition. Wiley (744 p).
Bjorksten, J., Tenhu, H., 1990. The crosslinking theory of aging — added evidence. Exp. Gerontol. 25 (2), 91–95. https://doi.org/10.1016/0531-5565(90)90039-5.
Blodgett, J.M., Theou, O., Howlett, S.E., Rockwood, K., 2017. A frailty index from common clinical and laboratory tests predicts increased risk of death across the life course. GeroScience 39 (4), 447–455.
Bondy, J.A., Murty, U.S.R., 1976. Graph Theory with Applications. Macmillan Press (270 p).
Farrell, S.G., Mitnitski, A.B., Rockwood, K., Rutenberg, A.D., 2016. Network model of human aging: frailty limits and information measures. Phys. Rev. E 94 (5), 052409. https://doi.org/10.1103/PhysRevE.94.052409.
Farrell, S. G., Mitnitski, A. B., Theou, O., Rockwood, K., & Rutenberg, A. D. (2018). Probing the Network Structure of Health Deficits in Human Aging. Cornell University Library, 1–16. https://doi.org/doi.org/https://doi.org/10.1101/270876.
Geisler, C., Braun, W., Pourhassan, M., Schweitzer, L., Glüer, C.-C., Bosy-Westphal, A., Müller, M., 2016. Age-dependent changes in resting energy expenditure (REE): insights from detailed body composition analysis in normal and overweight healthy Caucasians. Nutrients 8 (6), 322. https://doi.org/10.3390/nu8060322.
Hajizadeh, M., Mitnitski, A., Rockwood, K., 2016. Socioeconomic gradient in health in Canada: is the gap widening or narrowing? Health Policy 120 (9), 1040–1050. https://doi.org/10.1016/j.healthpol.2016.07.019.
Heckerman, D., Geiger, D., Chickering, D.M., 1995. Learning Bayesian networks: the combination of knowledge and statistical data. Mach. Learn. 20 (3), 197–243. https://doi.org/10.1023/A:1022623210503.
Hidalgo, C.A., Blumm, N., Barabási, A.-L., Christakis, N.A., 2009. A dynamic network approach for the study of human phenotypes. PLoS Comput. Biol. 5 (4), e1000353.
Hoffmann, P. (2016). Physics makes aging inevitable, not biology. Nautilus, Aging (36). Retrieved from http: //nautil.us/issue/36/aging/physics-makes-aging-inevitable-not-biology.
Højsgaard, S., Edwards, D., Lauritzen, S.L., 2012. Graphical Models with R, 1st ed. Springer, New York.
Howlett, S.E., Rockwood, M.R., Mitnitski, A., Rockwood, K., 2014. Standard laboratory tests to identify older adults at increased risk of death. BMC Med. 12 (1), 171. https://doi.org/10.1186/s12916-014-0171-9.
Kalisch, M., Mächler, M., Colombo, D., Maathuis, M. H., & Bühlmann, P. (2012). Causal inference using graphical models with the R package pcalg. J. Stat. Softw., 47 (11), 1–26. https://doi.org/10.18637/jss.v047.i11.
Kim, S., Welsh, D.A., Ravussin, E., Welsch, M.A., Cherry, K.E., Myers, L., Jazwinski, S.M., 2014. An elevation of resting metabolic rate with declining health in nonagenarians may be associated with decreased muscle mass and function in women and men, respectively. Journals of Gerontology-Series A Biological Sciences and Medical Sciences 69 (6), 650–656. https://doi.org/10.1093/gerona/glt150.
Kowald, A., Kirkwood, T.B.L., 1994. Towards a network theory of ageing: a model combining the free radical theory and the protein error theory. J. Theor. Biol. 168 (1), 75–94. https://doi.org/10.1006/jtbi.1994.1089.
Kriete, A., Sokhansanj, B.A., Coppock, D.L., West, G.B., 2006. Systems approaches to the networks of aging. Ageing Res. Rev. 5 (4), 434–448. https://doi.org/10.1016/j.arr.2006.06.002.
Lauritzen, S.L., 1996. Graphical models. In: Oxford Statistical Science Series, (312 p).
Lipsitz, L.A., 2016. The real secret of youth is complexity. Nautilus (36), 1–7 Aging.
Mitnitski, Arnold B., Graham, J.E., Mogilner, A.J., Rockwood, K., 2002. Frailty, fitness and late-life mortality in relation to chonological and biological age. BMC Geriatr. 2 (1), 1–8. https://doi.org/10.1186/1471-2318-2-1.
Mitnitski, A., Howlett, S.E., Rockwood, K., 2017a. Heterogeneity of human aging and its assessment. J. Gerontol. Ser. A Biol. Med. Sci. 72 (7), 877–884. https://doi.org/10.1093/gerona/glw089.
Mitnitski, A.B., Rutenberg, A.D., Farrell, S., Rockwood, K., 2017b. Aging, frailty and complex networks. Biogerontology 18 (4), 433–446. https://doi.org/10.1007/s10522-017-9684-x.
Morley, J.E., Vellas, B., Abellan van Kan, G., Anker, S.D., Bauer, J.M., Bernabei, R., Walston, J., 2013. Frailty consensus: a call to action. J. Am. Med. Dir. Assoc. 14 (6), 392–397. https://doi.org/10.1016/j.jamda.2013.03.022.
Pérez-Zepeda, Mario Ulises, Cesari, M., García-Peña, C., 2016a. Predictive value of frailty indices for adverse outcomes in older adults. Revista de Investigacion Clinica 68 (2), 92–98.
Pérez-Zepeda, M.U., Ávila-Funes, J.A., Gutiérrez-Robledo, L.M., García-Peña, C., 2016b. Frailty across age groups. J Frailty Aging 5 (1), 15–19.
Rockwood, K., Howlett, S.E., 2019. Age-related deficit accumulation and the diseases of ageing. Mech. Ageing Dev. 180, 107–116.
Rockwood, K., Mitnitski, A., 2007. Frailty in relation to the accumulation of deficits. J. Gerontol. A Biol. Sci. Med. Sci. 62, 722–727.
Rockwood, K., Hogan, D.B., Mac Knight, C., 2000. Conceptualisation and measurement of frailty in elderly people. Drugs Aging 17 (4), 295–302. https://doi.org/10.2165/00002512-200017040-00005.
Rockwood, K., Song, X., Mitnitski, A., 2011. Changes in relative fitness and frailty across the adult lifespan: evidence from the Canadian National Population Health Survey. CMAJ 183 (8), 487–494. https://doi.org/10.1503/cmaj.101271.
Rodríguez-Mañas, L., Féart, C., Mann, G., Viña, J., Chatterji, S., Chodzko-Zajko, W., Vega, E., 2013. Searching for an operational definition of frailty: a delphi method based consensus statement. The frailty operative definition-consensus conference project. Journals of Gerontology-Series A Biological Sciences and Medical Sciences 68 (1), 62–67. https://doi.org/10.1093/gerona/gls119.
Rutenberg, A.D., Mitnitski, A.B., Farrell, S., Rockwood, K., 2017. Unifying aging and frailty through complex dynamical networks. Experimental Gerontology, pii S0531 (June), 30482–30485. https://doi.org/10.1016/J.EXGER.2017.08.027.
Scutari, M., 2009. Learning Bayesian networks with the bnlearn R package. J. Stat. Softw. 35 (3), 1–22. https://doi.org/10.18637/jss.v035.i03.
Searle, S.D., Mitnitski, A., Gahbauer, E.A., Gill, T.M., Rockwood, K., 2008. A standard procedure for creating a frailty index. BMC Geriatr. 8, 1–10. https://doi.org/10.1186/1471-2318-8-24.
Sorkin, J.D., Muller, D.C., Andres, R., 1999. Longitudinal change in height of men and women: implications for interpretation of the body mass index: the Baltimore Longitudinal Study of Aging. Am. J. Epidemiol. 150 (9), 969–977. https://doi.org/10.1093/oxfordjournals.aje.a010106.
Spirtes, P., Glymour, C., 1991. An algorithm for fast recovery of sparse causal graphs. Soc. Sci. Comput. Rev. 9 (1), 62–72.
Taneja, S., Mitnitski, A.B., Rockwood, K., Rutenberg, A.D., 2016. Dynamical network model for age-related health deficits and mortality. Phys. Rev. E 93 (2), 022309. https://doi.org/10.1103/PhysRevE.93.022309.
Whitehead, J.C., Hildebrand, B.A., Sun, M., Rockwood, M.R., Rose, R.A., Rockwood, K., Howlett, S.E., 2014. A clinical frailty index in aging mice: comparisons with frailty index data in humans. Journals of Gerontology-Series A Biological Sciences and Medical Sciences 69 (6), 621–632. https://doi.org/10.1093/gerona/glt136.
Wong, R., Michaels-Obregon, A., Palloni, A., 2017. Cohort profile: the Mexican Health and Aging Study (MHAS). Int. J. Epidemiol. 46 (2), e2. https://doi.org/10.1093/ije/dyu263.
Zengarini, E., Ruggiero, C., Pérez-Zepeda, M.U., Hoogendijk, E.O., Vellas, B., Mecocci, P., Cesari, M., 2015. Fatigue: relevance and implications in the aging population. Exp. Gerontol. 70, 78–83. https://doi.org/10.1016/j.exger.2015.07.011.
Zengarini, E., Hoogendijk, E.O., Pérez-Zepeda, M.U., Ruggiero, C., Mecocci, P., Vellas, B., Cesari, M., 2016. Lack of energy and negative health-related outcomes in nursing home residents: results from the INCUR Study. J. Am. Med. Dir. Assoc. 17 (6), 525–529. https://doi.org/10.1016/j.jamda.2016.02.005.